RSC Advances

PAPER

View Article Online
View Journal | View Issue

Cite this: *RSC Adv.*, 2021, **11**, 2985

Self-healing solid polymer electrolyte based on imine bonds for high safety and stable lithium metal batteries†

Xiaoyan Cao,[a] Pengming Zhang,[a] Nanping Guo,[b] Yongfen Tong,*[a] Qiuhua Xu,[a] Dan Zhou[a] and Zhijun Feng[b]

Due to their low flammability, good dimensional stability and chemical stability, solid polymer electrolytes are currently attracting extensive interest for building lithium metal batteries. But severe safety issues such as cracks or breakage, resulting in short circuits will prevent their widespread application. Here, we report a new design of self-healing solid polymer electrolyte (ShSPE) based on imine bonds, fabricated from varying amounts of polyoxyethylenebis(amine) and terephthalaldehyde through a simple Schiff base reaction. Moreover, adding diglycidyl ether of bisphenol A improves the flexibility and high stretchability of the polymer electrolyte. The polymer networks exhibit good thermal stability and excellent self-healing characteristics. The ShSPE with the highest NH_2–PEG–NH_2 content (ShSPE-3) has an improved lithium ion transference number of 0.39, and exhibits an electrochemical stability up to 4.5 V *vs.* Li/Li^+. ShSPE-3 shows the highest ionic conductivity of 1.67×10^{-4} S cm^{-1} at 60 °C. Besides, the interfacial stability of ShSPE-3 is promoted and the electrolyte membrane exhibits good cycling performance with $LiFePO_4$, and the $LiFePO_4$/Li cell exhibits an initial discharge capacity of 141.3 mA h g^{-1}. These results suggest that self-healing solid polymer electrolytes are promising candidates for high safety and stable lithium metal batteries.

Received 27th November 2020
Accepted 26th December 2020

DOI: 10.1039/d0ra10035h

rsc.li/rsc-advances

Introduction

Li metal is considered as an optimal anode for its low reduction potential and high theoretical specific capacity (3860 mA h g^{-1}).[1–3] Thus the safety risks of conventional lithium-metal batteries using liquid electrolytes, which consist of low-molecular-weight organic carbonate solvents and lithium salt, still remain an important challenge.[4,5] After repeated charging and discharging, the uncontrollable lithium dendrite growth on lithium anodes might pierce the electrolytes and lead to internal short circuits, which would cause serious safety issues for lithium metal batteries.[6,7] On the other hand, poor stability is a long-standing problem preventing the practical application of Li metal anodes, which is fundamentally attributed to their fragile solid electrolyte interphase (SEI) layers that are intrinsically neither adaptable to the dynamic volume change nor self-healable after breakage. Therefore, improving the stability and safety is crucial to the development of high performance lithium metal batteries.[5,8] Some solid polymer electrolytes (SPEs), typically composed of lithium salts and polymer, have shown promise for solving the safety problems of lithium metal batteries.[9–11] However, solid electrolytes are inevitably bent, twisted and stretched when used in flexible batteries, which will lead to breakage and micro-cracks that result in short circuit and bring security risks.[12,13] Thus, it is urgent to develop a solid polymer electrolyte with self-healing properties to resolve the above mentioned problems to improve the safety and stability of the battery.

In nature, living kingdom utilizes self-healing ability to restore function and extend life.[14] Inspired by this, a series of self-healing materials have been studied to repair the damage of fracture interface through reversible chemical bond, hydrogen bond, ligand metal bond, and host guest interaction.[15–17] This idea promotes the rapid development of polymer materials with self-healing properties. Compared with traditional polymers, self-healing polymers show the ability to repair damaged areas *via* a physical or chemical processes.[18] SPEs based on self-healing materials can extend the lithium metal batteries lifetime and improve the cycling stability after crack or deformation.[19] In 2018, Zhou *et al.* fabricated a novel polymer electrolyte with intrinsic self-healability and high stretchability, which possesses good ionic conductivity at room temperature and excellent electrochemical and thermal stabilities.[20] Peng *et al.* report a new family of all-solid-state and flexible aqueous

[a]*School of Environmental and Chemical Engineering, Nanchang Hangkong University, 696 Fenghe South Avenue, Nanchang 330063, China. E-mail: tongyongfen@nchu.edu.cn; Fax: +86 791 83953373; Tel: +86 791 83953377*

[b]*School of Materials Science and Engineering, Nanchang Hangkong University, 696 Fenghe South Avenue, Nanchang 330063, China*

† Electronic supplementary information (ESI) available. See DOI: 10.1039/d0ra10035h

lithium ion batteries by designing aligned carbon nanotube sheets loaded with $LiMn_2O_4$ and $LiTi_2$ $(PO_4)_3$ nanoparticles on a self-healing polymer substrate as electrodes that can self-heal after breaking, and these self-healing batteries are demonstrated to be promising for wearable devices.[21] Li and Yang *et al.* applied a self-healing hydrogel with a double dynamic network comprising imine and borate ester linkages, which showed enhanced strength and mucoadhesive abilities because of the complimentary interpenetrating dynamic networks.[22] In addition, according to the self-healing mechanism, self-healing materials can be divided into extrinsic and intrinsic types.[23] Intrinsic self-healing materials use chemical and physical interactions, such as reversible chemical bonds or molecular diffusion to achieve repair damage interfaces.[24–26] When an external force (a change temperature, irradiation, light, PH, *etc.*) is received, these bonds can reversibly associate and dissociate, and some dynamic bonds at the fractured/damaged areas can be re-established.[27,28] For extrinsic self-healing materials, an extra repair agent is necessary to achieve self-healing. The imine bond (–C═N–) is a kind of reversible dynamic chemical bond, also known as Schiff base. The most common method to prepare imine bond compounds is reacted aldehyde or ketone with amine derivatives, generally speaking, the reaction can be divided into three equilibrium processes: imine condensation/hydrolysis, imine exchange, and imine metathesis, which show dynamic property for self-healing or recycling without catalyst. It can undergo rapid degenerative bond exchange without any significant side reactions and the advantage of solvent resistance.[29–32] In 2004, Brown and White, applied the microencapsulated dicyclopentadiene healing agent and Grubbs' Ru catalyst are incorporated into an epoxy matrix to produce a polymer composite capable of self-healing.[33] Zhang *et al.*, report an ultra-thin solid-state Li-ion electrolyte membrane facilitated by a self-healing polyimines polymer network, the malleability of polyamines allow for material flow to increase the density of the composite, and instill mechanical toughness.[34] In this study, we aim to prepare a serial of solid polymer electrolytes based on imine bond with self-healing properties and simultaneously possess excellent electrochemical performance.

Here, we propose the design of a flexible, self-healing and high mechanical strength solid polymer electrolyte (ShSPE) based on reversible imine bonds for all-solid-state lithium metal batteries. The ShSPE, composed of polyethylene glycol (PEG) strands and imine cross-linkers, was fabricated with diglycidyl ether of bisphenolA (DGEBA), terephthalaldehyde (TPA) separately thermal cross-linking with polyoxyethylenebis(amine) (NH_2–PEG–NH_2) at different molar ratios. The novel self-healing ShSPE were proposed to take advantages of the good ionic conductivity of EO unit, the fast self-healing properties of dynamic covalent imine bonds and the mechanical strength of the crosslinking of amines and epoxy groups in DGEBA. Due to the reversible of the dynamic imine bond, the as-prepared solid polymer electrolyte can self-repaire quickly after rupture or damage to ensure the inherent performance of the electrolyte. In addition, the epoxy resin structure will endow the electrolyte good adhesion properties, which will be conducive to form an effective contact between the electrolyte and the electrode, further improve the safety and stability of the battery.

Results and discussion

Preparation and characterization of ShSPE

A transparent and flexible solid polymer (ShSP, without Li salts) network was synthesized through cross-linking reaction by simply mixing diglycidyl ether of bisphenolA (DGEBA), terephthalaldehyde (TPA) and polyoxyethylenebis(amine) (NH_2–PEG–NH_2) in acetonitrile (Fig. 1a). In this system, the active amine groups on the linear NH_2–PEG–NH_2 segment can react with aldehydes of TPA to form polymer structure containing imine bonds under heating conditions. The reversibility of imine bond endows polymer structure with self-healing ability. When the polymer is subjected to internal or external forces, it will rapidly self repair under the action of reversible dynamic covalent bond to restore its original shape and function.[35] The idealized reaction mechanism diagram is shown in Fig. 1b, mainly manifested as condensation reaction of amine groups on the NH_2–PEG–NH_2 with aldehyde groups of TPA can form segments containing imine bonds, which indicated as red line segments in the Fig. 1b. Besides, epoxy groups in the DGEBA were reacted with amino group to achieve the covalent structure as purple part in Fig. 1b. By embedding reversible imine bonds into epoxy polymer network, the two parts are crosslinked to form a semi-interpenetrating polymer structure.[36,37] It is worth noting that NH_2–PEG–NH_2 segment has a great influence on the film-forming property of the electrolyte. When the molar ratio of NH_2–PEG–NH_2 is above 4, no self-standing polymer electrolyte films are observed and the electrolyte is gelatinous, indicating that the feed ratio of the polymerization components will directly affect the independent film formation. Therefore, the molar ratio of TPA, DGEBA and NH_2–PEG–NH_2 is 1/2/(1–3) is used to study various properties.

As shown in Fig. 2a and b excellent flexibility, transparent and self-standing polymer electrolyte films can be prepared by fusing polyoxyethylenebis (amine), terephthalaldehyde (TPA) with diglycidyl ether of bisphenol A. The thickness of ShSPE which were used in the lithium metal batteries is approximately 30∼80 μm. Because the film is relatively thin and soft, the average value is taken through multiple parallel measurements with a spiral micrometer (Fig. 2c). The surface morphology of the electrolytes film is also shown in Fig. 2d, a smooth surface and compact structure without phase separations are found, illustrating that each polymer chain segment has good compatibility.

In order to investe the structure of polymer, Fourier transform infrared (FT-IR) analysis was used to confirm the successful formation of dynamic covalent polymer.

According to the previous design, the ShSP-3 with dynamic imine bonds was obtained by the condensation of amino group in NH_2–PEG–NH_2 and aldehyde group in TPA. Fig. 3a shows the FT-IR spectra of DGEBA, TPA and ShSP-3. The peaks at 1695 cm^{-1} correspond to the stretching vibration of C═O from aldehyde group. Compared with the spectrum of TPA, the

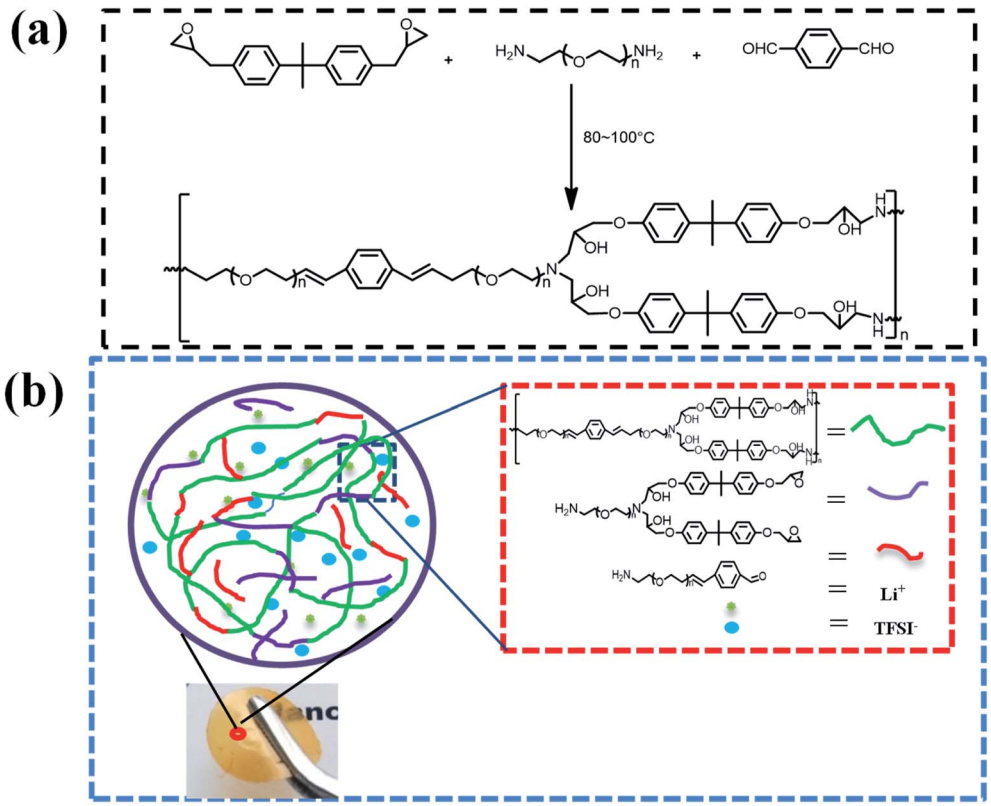

Fig. 1 Schematic illustration (a) and mechanism diagram (b) for the preparation of ShSPE network.

absorption band of aldehyde group disappeared for ShSP-3, and a new –N═CH– bond at 1650 cm^{-1} appeared, indicating the successful polymerization of ShSP-3.[38,39] Simultaneously, the amine group can attack epoxy structure to break the epoxy groups (at 912 cm^{-1}) in the DGEBA, and the hydroxyls are created after ring-opening reaction.[40]

Since the ionic conductivity of the polymer electrolyte is closely related to the morphology of the polymer, the X-ray diffraction (XRD) study of the self-healable ShSP and the ShSPE are carried out (Fig. 3b). Generally, the sharp reflections at $2\theta = 19.2°$ and 23.4° are corresponding to the crystallinity of PEG segment. From ShSP-1 to ShSP-2 to ShSP-3, the intensity of these peaks of the PEG increases, implying that the degree of crystallization decreases as the NH_2–PEG–NH_2 content decreases. Further introducing the LiTFSI, the sharp peaks disappeared. This means that the lithium salt acts as a plasticizer can inhibit the crystallization of EO chain, and the solid polymer electrolytes are amorphous, which are helpful to improve the ionic conductivity of ShSPE.[6] Moreover thermogravimetric analysis (TGA) and the differential scanning calorimetry (DSC) further reveals the designed ShSPE possesses an amorphous structure with good thermal stability (Fig. 4a) and a lowest glass transition temperature (Fig. 4b).

Thermal analysis of ShSPE

The thermal stability of electrolytes is of import for lithium metal battery and the decomposition temperature of ShSP-3 and ShSPE samples was assessed by thermogravimetric analysis (TGA). The results were shown in Fig. 4a. It could be clearly seen that polymers without Li salts (ShSP-3) show negligible weight loss until temperature reaches up to 300 °C, and all the ShSPEs show high decomposition temperature (~350 °C). This phenomenon reveals that the ShSPE are thermostatically stable even under high-temperature circumstances, indicating the polymer electrolyte are highly stable and safe to meet the requirement of using in very high temperature for lithium metal battery.

Fig. 4b shows the DSC traces of virgin polymer after NH_2–PEG–NH_2 and TPA, DGEBA polymerization reaction and polymer electrolytes in the temperature range of −80 to 100 °C. An obvious peak of ShSP-3 curve at 50.4 °C are associated to the melting temperature (T_m) of PEG. The glass transition temperature (T_g) of ShSPE-3~1 show relative lower T_g in the temperature range of −33.2 to −28.2 °C and the peak of T_m disappear, indicating that the electrolytes are amorphous, which is according with the analysis of XRD. This result portends LiTFSI added into the polymers system is not only responsible for ion transmission, but also act as plasticizer to inhibit polymer crystalline in the ShSPE system. Such low T_g indicated that the ShSPE is highly flexible and possess good segmental motion, which is benefit to the lithium ion transport and movement.[41]

In order to further prove the thermal stability of the electrolyte, the traditional Celgard separator membrane was compared with ShSPE-3 in combustion and dimensional stability test. The results are shown in Fig. 5a and Fig. 5b,

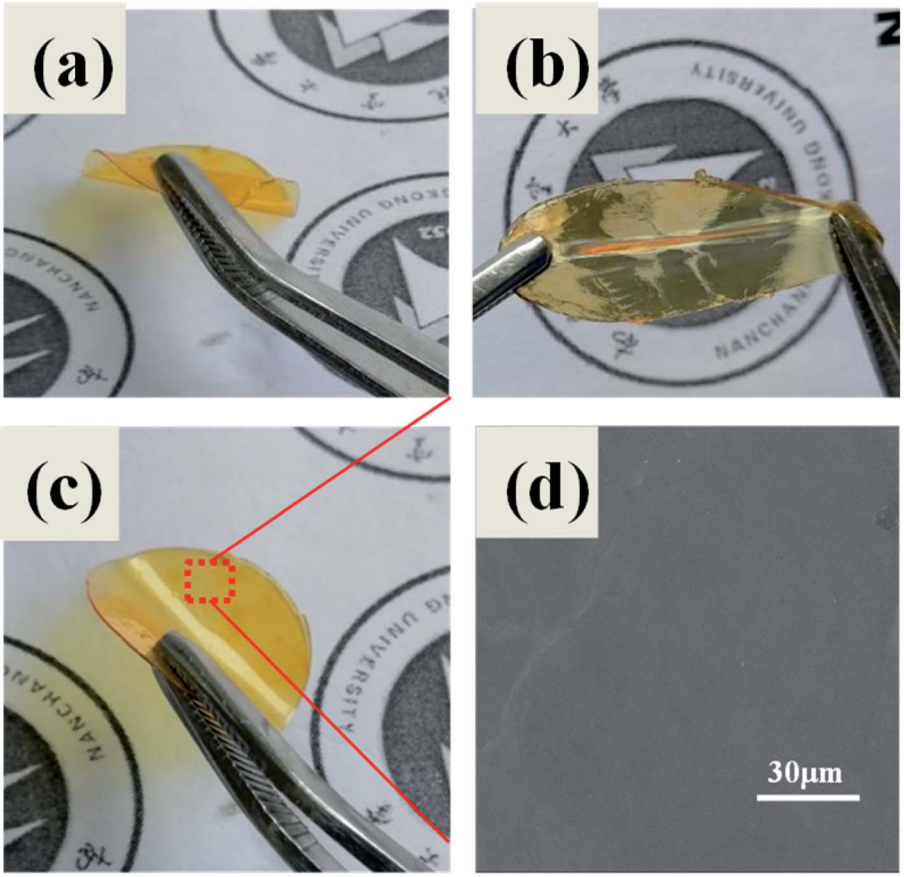

Fig. 2 Photographs for ShSPE (a–c) and SEM image of the surface for ShSPE (d).

respectively. When the Celgard separator was ignited, it will completely burn within 2 s, which is due to the presence of combustible substances such as polyethylene and polypropylene.[42] However, ShSPE-3 only appears edge curl after burning on fire for 1 minute. The results show that ShSPE has better fire retardancy than traditional Celgard film. In addition, heat retardancy of ShSPE and Celgard separator were also measured for comparition. Fig. 5b records the photographic images of ShSPE-3 and Celgard from 100 °C to 180 °C. It can be clearly seen that Celgard separator membrane begin to shrink at 100 °C and gradually become transparent, while the color and size of ShSPE-3 films are hardly affected by temperature. This combustion and dimensional stability contrast test further demonstrates the high heat resistance of ShSPE-3 film, which is

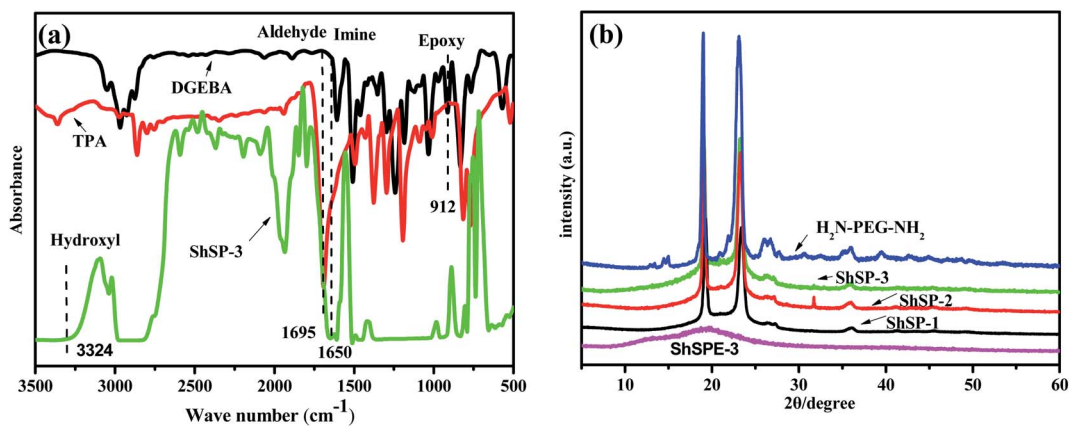

Fig. 3 FT-IR spectra of DGEBA, TPA and ShSP-3 elastomer (a) and XRD spectra (b) for NH_2–PEG–NH_2, polymers without Li salts (ShSP-1, 2, 3) and ShSPE-3.

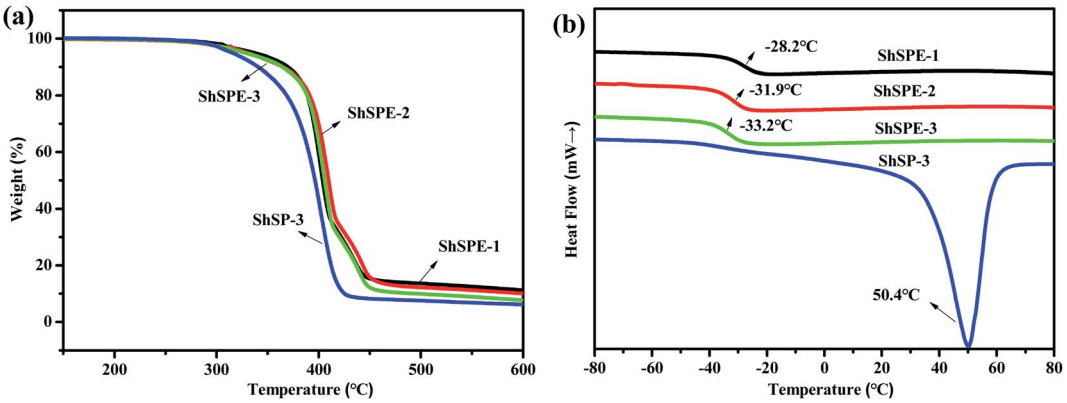

Fig. 4 TGA (a) and DSC (b) curves for self-healable solid polymers without Li salts (ShSP-3) and the self-healable polymeric electrolyte at different molar ratios.

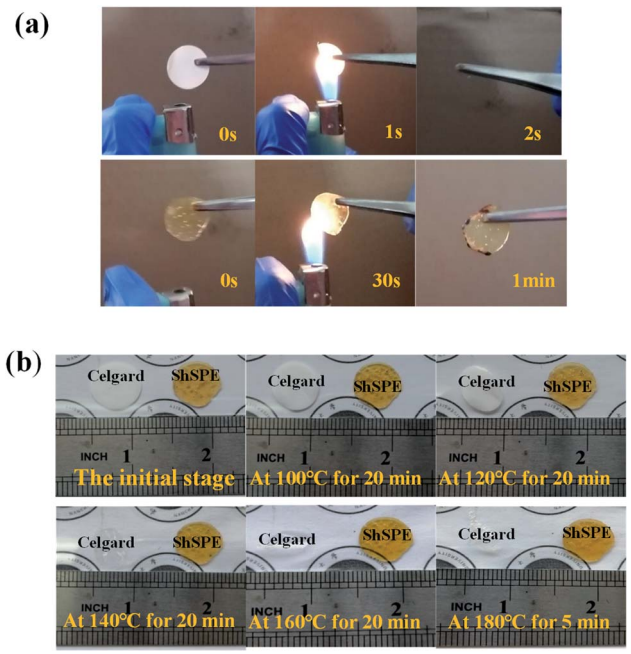

Fig. 5 Photographic images (a) of the flammability test of Celgard and ShSPE-3 and heated at a different temperature (b) under normal atmospheric conditions.

suitable for the development of high temperature lithium metal battery.[43]

Stretchability and self-healing properties of ShSPE

With the emergence of flexible and wearable energy storage devices, the scalability properties of materials are required for the practical application. Some materials will easily fracture under stretching or bending.[20] The stretchability properties of the ShSPE-3 were measured by tensile test. It is gratifying that the ShSPE-3 reported here exhibits excellent stretchability properties (Fig. S1†). The mechanical strength of the polymer electrolyte benefited from the covalent bond formed by the ring-opening reaction between the amino group contained in NH_2–PEG–NH_2 and the epoxy structure in DGEBA.[44] The good stretchable capabilities are favor to improve the safety of the solid polymer electrolytes.

In order to study the healing efficiency of ShSPE, we further studied the healing rate at different temperatures (Fig. 6a). The samples were cut into two pieces and healed at 25 °C, 60 °C and 80 °C, as represented in Fig. 6b–d respectively. This is attribute to the dynamic reversible imine bonds which can undergo both dissociative (imine hydrolysis and re-formation) and associative (imine–amine exchange and imine condensation) reactions between amine groups in the NH_2–PEG–NH_2 backbone and aldehyde groups of TPA or imine-containing polymer network.[36] Two separated ShSPE-3 samples were fully recovered after contacted for 30 minutes at 25 °C without any external stimuli, the two halves fused into a single entity. To further confirm the self-healing ability, the healing process of cut ShSPE-3 film was observed before and after healing by the microscope, as shown in Fig. 6e. There was no defect in the recovery membrane, which strongly shows that the electrolytes poseess excellent self-healing ability. The ShSPE-3 elastomer of the self-healing process is schematically presented in Fig. 6f. It is worth mentioning that the repaired samples with a strong enough bond still show good stretch properties without cracks on the original damage, indicating the ShSPE were healed effectively to the original entirety. This is ascribe to the existence of reversible imine bond din the polymer network. Thus, it can conclude that high concentrations of NH_2–PEG–NH_2 may increase the chance of meeting aldehyde groups and further promote the imine exchange reactions, thereby increasing the possibility of forming imine bonds. Simultaneously, self-healing rate has been greatly improved at elevated temperature. The cut interface became fully recovered within 10 min at 60 °C and only within 5 min at 80 °C, which could be ascribed to the higher flexibility and mobility of polymer chains at high temperature.

Interfacial stability and adhesivity of electrolyte/electrodes

The interface compatibility and stability significantly affect the cycle performance and rate performance of all solid-state lithium metal battery. The solid–solid contact in solid-state

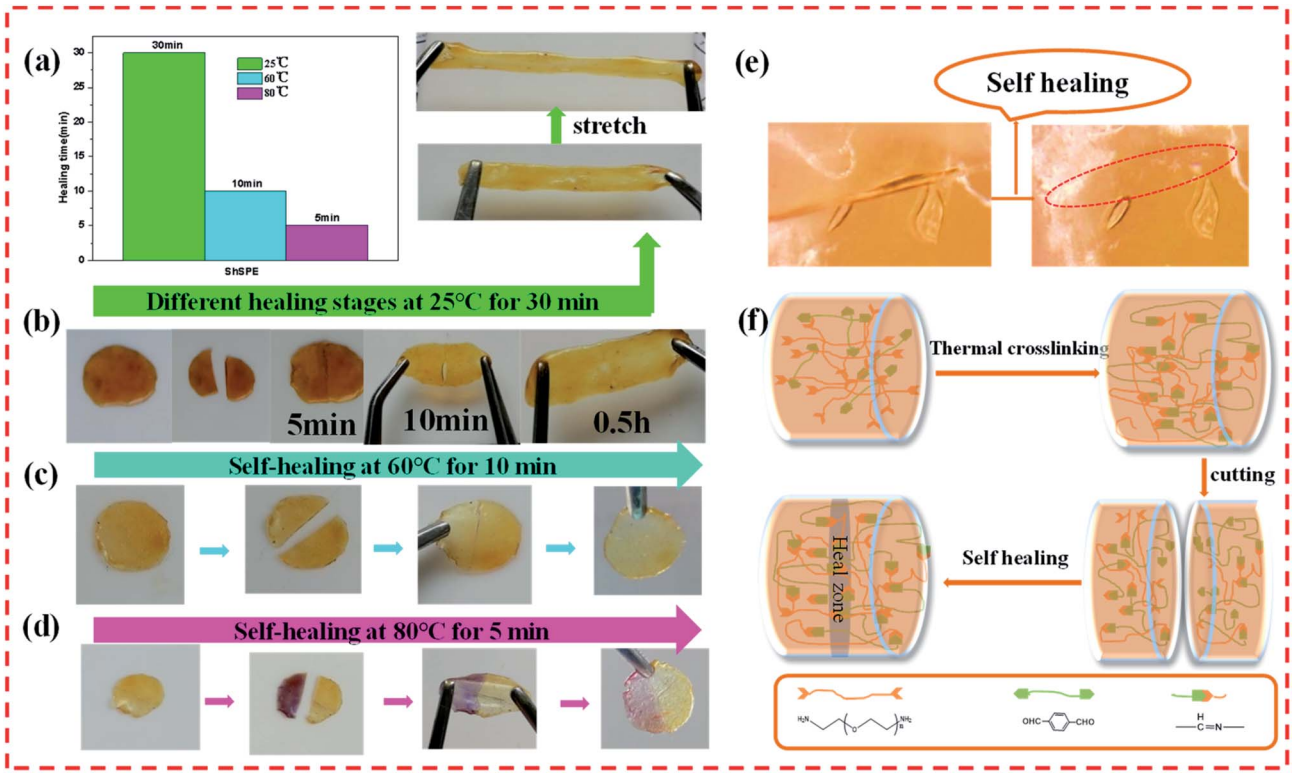

Fig. 6 Self-healing time of ShSPEs at different temperatures (a), the optical images showing the self-healing process of the ShSPE-3 pieces under ambient conditions (b), 60 °C (c), 80 °C (d), optical microscope images of self-healing process for polymer films (e) and schematic illustration of the self-healing process (f).

lithium metal battery between electrode and solid electrolyte has higher contact resistance than solid–liquid contact.[45] Therefore, the poor interface problem will affect the electrochemical performance of the battery, and the problem becomes even worse for flexible and wearable electronic device under deformation conditions. By observing the SEM images of cross for Li/ShSPE-3/$LiFePO_4$ full cells after 5 cycles of deposition/stripping (Fig. 7a), it can clearly see that the $LiFePO_4$ and ShSPE-3 can be closely bonded and the thickness of ShSPE-3 is about 40 μm. Fig. 7b shows the process of lithium ion stripping/plating on lithium metal. Generally, the poor contact between the electrolyte and the electrode will lead to the uneven deposition for lithium ion on the lithium anode during the process of Li plating pattern. When a uniform and stable SEI layer is formed between the electrode and the electrolyte, the ShSPE with homogeneous interfacial contact and high-efficiency Li^+ diffusion manner at the surface of Li anode will be in favor of a compact and dense Li plating pattern. Element mapping also confirmed a homogenously SEI layer on the Li metal anodes after 5 cycles of deposition/stripping (Fig. S2a†).

The stability and interface contact performance of the electrolyte and lithium metal can be further observed by the

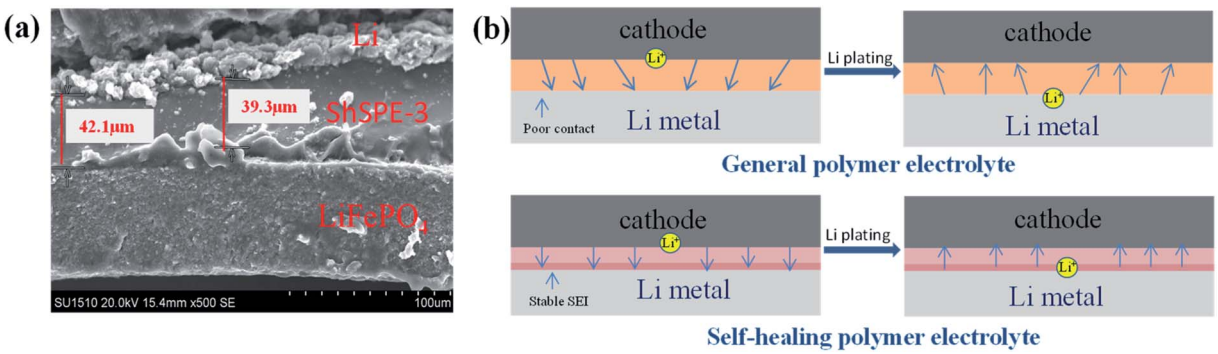

Fig. 7 Cross-sectional SEM images of the Li/ShSPE-3/$LiFePO_4$ (a) and schematic illustration of Li plating of general and self-healing polymer electrolytes on Li metal (b).

adhesive test for electrolyte. Here, the adhesive strength between ShSPE-3 and metal surface is measured, and the results are shown in Fig. S2b.† The membrane was coated on a metal surface with the diameter of 18 mm and the thickness of film was less than 1 mm. Then a metal ruler was covered on electrolyte surface, and two metal surface were bonded together under pressure. The experimental results show that the metal surface with ShSPE-3 can easily support the weight of 200 g. It shows that ShSPE-3 has good adhesion properties. The excellent adhesion performance ensures the interface stability and good compatibility between ShSPE and electrode, then improves the safety and stability of battery.

Electrochemical properties of ShSPE

In order to get the ShSPE with the best electrochemical performance, a series of ShSPE with different ratios of base materials (NH_2–PEG–NH_2 and TPA, DGEBA) and different molar ratio of lithium salt were assembled with SS/ShSPE/SS blocking cells for EIS measurement in a temperature range from 20 °C to 80 °C and Li/ShSPE/SS cells for LSV measurement at room temperature. Fig. 8a shows the temperature dependence of ionic conductivity of ShSPE while maintaining the molar ratio of EO/Li^+ at 16 : 1. It can be see that the ionic conductivities value of all the electrolytes increase with increasing temperature, means that the conductivity of polymer electrolyte based on PEG is related to the movement of polymer chains and lithium ions relatively easy migrate in the flexibly PEG segments. The ionic conductivity values of ShSPEs were 5.75×10^{-5}, 8.13×10^{-5}, and 1.67×10^{-4} S cm^{-1} at 60 °C for ShSPE-1, ShSPE-2, and ShSPE-3, respectively. ShSPE-3 with the highest content of NH_2–PEG–NH_2 possess the highest ionic conductivity. Beyond this critical point, the polymer can't effectively form a self-supporting film. The conductivity shows a clear dependency on PEG concentration for the salt dissociation ability of the ethylene oxide units. Therefore, the ionic conductivity of ShSPE increases with the increase of PEG content. Meanwhile, the lithium ions per ethylene oxide units are in the polymer matrix also affects the ionic conductivity of the electrolytes. It can be seen from Fig. 8b that the conductivity reaches the maximum when the oxygen-lithium ratio of ShSPE-

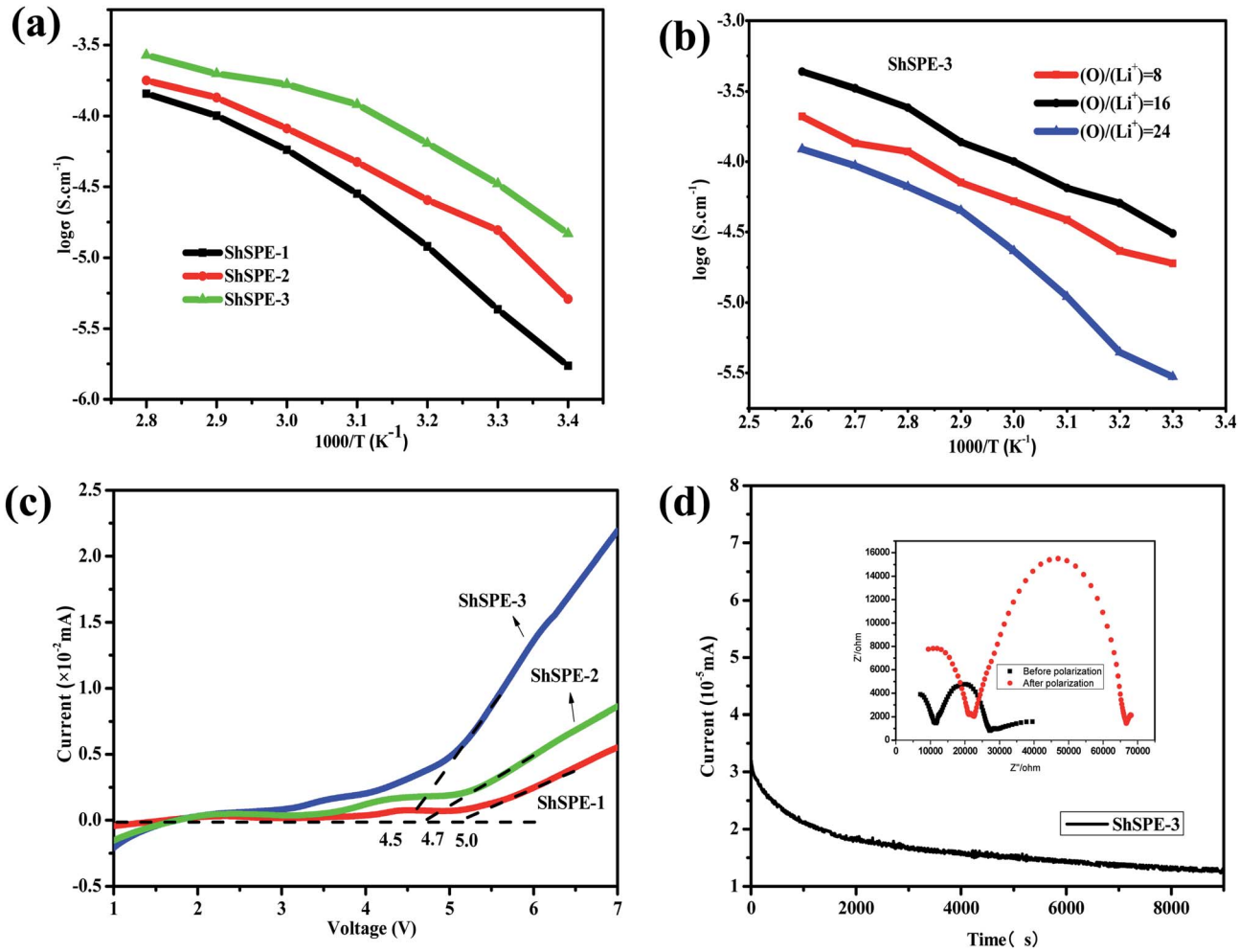

Fig. 8 The temperature dependence of ionic conductivity for ShSPEs with different content of PEG (a), and different oxygen–lithium ratio (b), LSV curves of ShSPEs at room temperature (c), chronoamperometry of the Li/ShSPE-3/Li cell (d) (the inset shows the AC impedance spectra before and after polarization at room temperature).

3 is 16/1. In principle, the higher of lithium concentration is benefit to improve the ionic conductivity. But further increase of the concentration of lithium salt, it will lead to the aggregation of salt, which is not conducive to it move and result in reducing the ion transport.[46] Fig. S3† shows the EIS plot of the SS/ShSPE-3/SS cell at temperatures from 20 to 80 °C. As the temperature rises, the bulk impedance of the electrolyte gradually becomes smaller, the ion transmission speeds up, and the ion conductivity increases. Linear Sweep Voltammetry (LSV) was performed to evaluate the electrochemical stability window of the ShSPE (Fig. 8c). The oxidative degradation take place at around 5.0 V, 4.7 V and 4.5 V for ShSPE-1, ShSPE-2 and ShSPE-3, respectively, which means that the self-healing polymer electrolytes can be used in practical applications for lithium metal batteries.

The lithium ion transference number (t_{Li^+}) is also an important parameter for solid polymer electrolytes. The chronoamperometry curve and the electrochemical impedance spectra before and after steady-state of Li/ShSPE-3/Li cell are shown in Fig. 8d. The calculated t_{Li^+} was 0.39 which is in good agreement with reported value for PEO/LiTFSI system, indicating that the ShSPE provide more ion diffusion channels and promote ion transport. The comprehensive electrochemical properties of the designed ShSPE is suitable for solid-state lithium metal batteries.

Full cells were assembled for an assessment with lithium-metal as the anode and $LiFePO_4$ as the cathode under practical conditions. The charge/discharge performance of Li|ShSPE-3|$LiFePO_4$ battery illustrated between 2.5 V and 4.2 V at a rate of 0.1C and 60 °C were plotted in Fig. 9a. The initial discharge capacities were 141.3 mA h g^{-1} and the coulombic efficiency approach to 96.8%. The typical plateaus shown in the process of charge/discharge demonstrate a reversible electrochemical reaction for the battery. Fig. 9b shows the cycling performance of Li|ShSPE-3|$LiFePO_4$ cell at 60 °C. The batteries retain good specific capacity (120.4 mA h g^{-1}) and excellent coulombic efficiency (about 97.7%) after 50 cycles at a 0.1 C-rate. The good cycling performance can be due to the good contact between the ShSPE and the electrode. In order to study the battery performance of the self-healing electrolyte, we also provided cycle performance of the Li|ShSPE|$LiFePO_4$ battery based on healed ShSPE-3 from the cut sample at 0.1C rate (Fig. S4†). It is worth mentioning that lithium metal battery can still charge and discharge. The initial discharge capacities was 137.7 mA h g^{-1} at 60 °C and the capacity of 119.34 mA h g^{-1} is still retained after 50 cycles, which is comparable to the discharge performance of as-prepared electrolytes. This suggests that the healed electrolyte has no effect on the performance of the battery.

In order to systematically study the battery performance of the all-solid polymer electrolyte prepared, the properties of several common PEG polymer electrolytes are compared and shown in Table S1.† It can be clearly seen that the electrochemistry properties of the ShSPE prepared in this paper is similar to that reported in literature.

To further investigate the practical applications of ShSPE in electronic devices, all-solid-state cell using pristine ShSPE-3 are used to light up yellow light-emitting diode (LED) lamp under a normal condition Fig. 10a. To further underline the excellent safety issue, the cell used healed ShSPE-3 was shown in Fig. 10b. It was observed that all the cell can power the LED lamp and the brightness of the lamp has almost no effect before and after healing. This is an evidence to prove that lithium metal batteries based on ShSPE display improvements in safety and longevity.

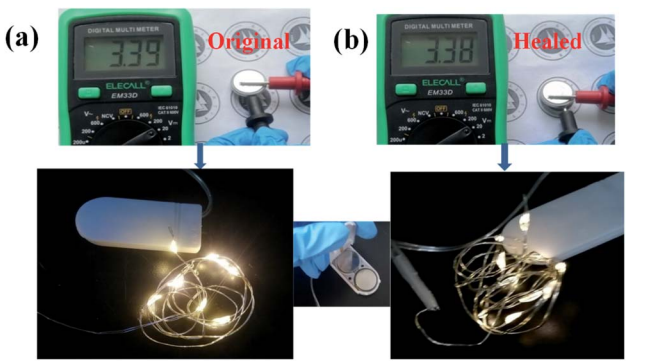

Fig. 10 Photo image and open circuit voltage of pristine and healed ShSPE-3 based Li/LFP battery (a), the photographs of the lightened LED devices before and after self-healing (b).

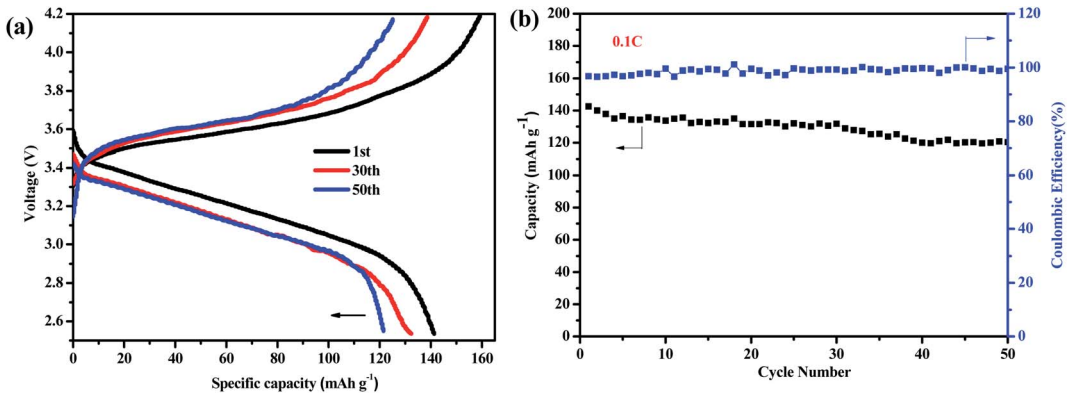

Fig. 9 Charge–discharge curves of ShSPE-3 based $LiFePO_4$/Li cell for 0.1C at 60 °C with the voltage range from 2.5 to 4.2 V (a), cycling performance of the LFP/ShSPE-3/Li cell (b).

Conclusion

In summary, we have successfully developed a self-healing and highly stretchable solid polymer electrolyte (ShSPE) based on imine bonds *via* a Schiff base reaction and ring-opening polymerization technique. The ShSPE can be simply self-healed by reattached the broken interfaces and show good tensile properties, which has been successfully used as the separator in Li metal batteries. Furthermore, the interface of the battery based on ShSPE exhibits high chemical stability during the deposition/dissolution process, which is benefit from its good contact with the electrode. Deployment of ShSPE as electrolytes in Li/ShSPE-3/LFP cell shows that they enable good cycling stability and high cell-level coulombic efficiency. More importantly, solid-state lithium metal batteries based on cut-healing ShSPE also present excellent electrochemical performance and safety characteristic. Thus, the outstanding performance of ShSPE developed in this work make it one of the most promising electrolytes for flexible and wearable lithium metal batteries with highly improved safety and stability.

Conflicts of interest

There are no conflicts to declare.

Acknowledgements

This work was supported by the National Natural Science Foundation of China (21404054, 22065025 and 21965023) and Natural Science Foundation of Jiangxi Province (20192BAB206013 and 20202BBEL53035).

References

1 J. M. Tarascon and M. Armand, *Nature*, 2001, **414**, 359.
2 D. Lin, Y. Liu and Y. Cui, *Nat. Nanotechnol.*, 2017, **12**, 194.
3 W. Xu, J. Wang, F. Ding, X. Chen, E. Nasybulin, Y. Zhang and J. Zhang, *Energy Environ. Sci.*, 2014, **7**, 513.
4 K. Xu, *J. Chem. Rev.*, 2004, **104**, 4303.
5 X. Cui, Y. Chu, L. Qin and Q. Pan, *ACS Sustainable Chem. Eng.*, 2018, **6**, 11097.
6 N. Wu, Y. Shi, S. Lang, J. Zhou, J. Liang, W. Wang, S. Tan, Y. Yin, R. Wen and Y. Guo, *Angew. Chem., Int. Ed.*, 2019, **58**, 18146.
7 J. Qian, W. Henderson, W. Xu, P. Bhattacharya, M. Engelhard, O. Borodin and J. Zhang, *Nat. Commun.*, 2015, **6**, 6362.
8 B. Zhou, Y. Jo, R. Wang, D. He, X. Zhou, X. Xie and Z. Xue, *J. Mater. Chem. A*, 2019, **7**, 10354.
9 T. Dong, J. Zhang, Q. Zhou, G. Xu, J. Chai, H. Du, L. Wang, H. Wen, X. Zang, A. Du and G. Cui, *Energy Environ. Sci.*, 2018, **11**, 1197.
10 H. Zhang, L. Cui, J. Zhang, J. Ma, J. Xu, T. Dong and G. Cui, *Electrochem. Energy Rev.*, 2019, **2**, 128.
11 Q. Wang, L. Cui, Q. Zhou, X. ShangGuan, X. Du, S. Dong, L. Qiao, S. Huang, X. Liu and G. Cui, *Energy Storage Mater.*, 2020, **25**, 756.
12 Z. Zhang, X. Jin, G. Sun, H. Yang, G. Zhang, Y. Xiao, J. Gao and L. Qu, *J. Mater. Chem. A*, 2018, **6**, 19463.
13 W. D. Richards, T. Tsujimura, L. J. Miara, Y. Wang, J. C. Kim, S. P. Ong, I. Uechi, N. Suzuki and G. Ceder, *Nat. Commun.*, 2016, **7**, 11009.
14 Y. Gu and N. S. Zacharia, *Adv. Funct. Mater.*, 2015, **25**, 3785.
15 K. Imato, M. Nishihara, T. Kanehara, Y. Amamoto, A. Takahara and H. Otsuka, *Angew. Chem.*, 2012, **51**, 1164.
16 J. Mei, X. Jia, J. Lai, Y. Sun, C. Li, J. Wu, Y. Cao, X. You and Z. Bao, *Macromol. Rapid Commun.*, 2016, **37**, 1667.
17 C. K. Tee, C. Wang, R. Allen and Z. Bao, *Nat. Nanotechnol.*, 2012, **7**, 825.
18 K. Liu, X. Pan, L. Chen, L. Huang, Y. Ni, J. Liu, S. Cao and H. Wang, *ACS Sustainable Chem. Eng.*, 2018, **6**, 6395.
19 X. Zeng, Y. Yin, N. Li, W. Du, Y. Guo and L. Wan, *J. Am. Chem. Soc.*, 2016, **138**, 15825.
20 B. Zhou, D. He, J. Hu, Y. Ye and H. Peng, *J. Mater. Chem. A*, 2018, **6**, 11725.
21 Y. Zhao, Y. Zhang, H. Sun, X. Dong, J. Cao, L. Wang, Y. Xu, J. Ren, Y. Hwang and I. H. Son, *Angew. Chem., Int. Ed.*, 2016, **128**, 14596.
22 Y. Li, L. Yang, Y. Zeng, Y. Wu, Y. Wei and L. k. Tao, *Chem. Mater.*, 2019, **31**, 5576.
23 J. Chen, F. Li, Y. Luo, X. Ma and Z. Luo, *J. Mater. Chem. A*, 2019, **7**, 15207.
24 J. Dahlke, R. Tepper, R. Geitner, S. Zechel, J. Vitz, R. Kampes, P. J. opp, M. D. Hager and U. S. Schubert, *J. Polym. Sci.*, 2018, **9**, 2193.
25 N. Roy, B. Bruchmann and J.-M. Lehn, *Chem. Soc. Rev.*, 2015, **46**, 3786.
26 Z. Wang, X. Lu, S. Sun, C. Yu and H. Xia, *J. Mater. Chem. B*, 2019, **7**, 4876.
27 Y. Cao, T. G. Morrissey, E. Acome, S. I. Allec, B. M. Wong, C. Keplinger and C. Wang, *Adv. Mater.*, 2016, **29**, 1605099.
28 C. Wang, N. Liu, R. Allen, J. B.-H. Tok, Y. Wu, F. Zhang, Y. Chen and Z. Bao, *J. Adv. Mater.*, 2013, **25**, 5785.
29 H. Zhang, D. Wang, W. Liu, P. Li, J. Liu, C. Liu, C. Zhang, N. Zhang and J. Xu, *J. Polym. Sci., Part A: Polym. Chem.*, 2017, **55**, 2011.
30 J. Ren, B. Ni, H. Liu, Y. Hu, X. Zhang and T. Masuda, *Polym. Chem.*, 2019, **10**, 1238.
31 M. Ciaccia, R. Cacciapaglia, P. Mencarelli, L. Mandolini and S. D. Stefano, *J. Chem. Sci.*, 2013, **4**, 2253.
32 W. Zou, J. Dong, Y. Luo, Q. Zhao and T. Xie, *J. Adv. Mater.*, 2017, **29**, 1606100.
33 E. Brown, S. White and N. Sottos, *J. Mater. Sci.*, 2004, **39**, 1703.
34 J. M. Whiteley, P. Taynton, W. Zhang and S. Lee, *Adv. Mater.*, 2015, **27**, 6922.
35 Y. Zhao, Y. Zhang, H. Sun, X. Dong, J. Cao, L. Wang, Y. Xu, J. Ren, Y. Hwang and I. H. Son, *Angew. Chem.*, 2016, **128**, 14596.
36 S. Zhao and M. M. Abu-Omar, *Macromolecules*, 2018, **51**, 9816.
37 C. Xu, W. Zhan, X. Tang, F. Mo, L. Fu and B. Lin, *Polym. Test.*, 2018, **66**, 155.

38 J. Ren, Y. Zhu, H. Xuan, X. Liu, Z. Lou and L. Ge, *RSC Adv.*, 2016, **6**, 115247.
39 P. Wang, L. Yang, B. Dai, Z. Yang, S. Guo, G. Gao, L. Xu, M. Sun, K. Yao and J. Zhu, *Eur. Polym. J.*, 2020, **123**, 109382.
40 Y. H. Jo, B. Zhou and K. Jiang, *J. Polym. Sci.*, 2019, **10**, 6561.
41 Z. Xue, D. He and X. Xie, *J. Mater. Chem. A*, 2015, **3**, 19218.
42 Y. Zhu, F. Wang, L. Liu, S. Xiao, Y. Yang and Y. Wu, *Sci. Rep.*, 2013, **3**, 3187.
43 S. Feng, D. Shi, F. Liu, L. Zheng, J. Nie, W. Feng, X. Huang, M. Armand and Z. Zhou, *Electrochim. Acta*, 2013, **93**, 254.
44 Q. H. Yang, *J. Adv. Mater.*, 2017, **29**, 1604460.
45 X. Cheng, T. Hou, R. Zhang, H. Peng, C. Zhao, J. Huang and Q. Zhang, *J. Adv. Mater.*, 2016, **28**, 2888.
46 J. Zhang, C. Ma, J. Liu, L. Chen, A. Pan and W. Wei, *J. Membr. Sci.*, 2016, **509**, 138.